ucc

Coláiste na hOllscoile Corcaigh, Éire
University College Cork, Ireland

Department of Applied Mathematics,
University College Cork,
Ireland

AM4090 - Research Project

Final report

Modelling photon correlations from quantum dots.

Eoin Murray

110367833

Supervisor: Dr. Andreas Amann.

April 25, 2014.

Declaration

This report was written entirely by the author, except where stated otherwise. The source of any material not created by the author has been clearly referenced. The work described in this report was conducted by the author, except where stated otherwise.

Abstract

Research on the practical realisation of quantum computing and quantum information science is proceeding at a tremendous pace. The associated challenges are being addressed by various technologies. Quantum dots (QDs) are a promising technology to act as the active photonic qubit source. Quantum dots are commonly referred to as "artificial atoms" due to their discrete energy levels and few carrier confinement. They are attractive because they allow on demand qubits and can be manufactured using conventional semiconductor foundry technologies. An inexpensive solid state device capable of generating single and entangled qubits on demand would be a great asset in exploring practical quantum technologies.

Understanding the energetic fine-structure of the quantum dot is vitally important. Typically correlation measurements on the emitted photons are done to determine the order of a particular decay cascade through the fine structure. In this report a strict method of modeling the correlations based on hypothesised fine-structures is presented. First and introduction to quantum dots is presented along with an introduction to stochastic processes. Then the relationship between the stochastic model and the measured correlations is derived. Lastly a preliminary discussion is presented on applying the model to measured data.

Electrons and holes are created in or near the dot by electro- or photo-excitation. Electrons are excited into the conduction band and holes are left in the valence band. An e-h pair is referred to as an exciton. Typically, mobile carriers are created in the bulk material by above band excitation and they relax into different confinement potentials in the heterostructure. The QD will normally be the lowest energy confinement.

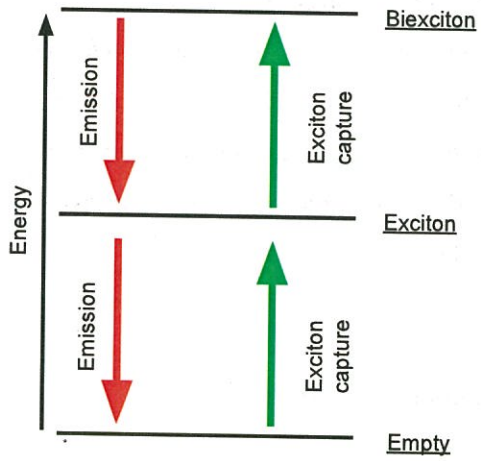

Figure 2: Fine structure of the biexciton.

In the ideal case, a typical population process of the QD will go as follows. First an e-h pair, known as an exciton, is captured in the QD. It either decays optically to the ground state, or it survives long enough that another exciton is captured. When two excitons exist in the QD, it is known as a biexciton, this biexciton will likely survive (since the confinement energy to capture a third is typically much higher) until it decays optically to the exciton state, which will then decay optically to the ground state. In this process two photon pairs are emitted from the QD. The fine structure transition process is shown schematically in Figure 2. These photons are predicted to be entangled due to the indistinguishability of two excitons [1]. Due to the on-demand nature in which they are created, they are good candidates for quantum computation [4]. They are typically separated in energy, and can be discriminated by spectroscopy. By simply ignoring the first biexciton photon the QD can be though of as a single photon emitter [3, 6]. This is also a very useful property of the QD, as single photon emission has a range of applications in quantum cryptography [5].

If the number of electrons and holes in the bulk material are balanced, electrons and holes

will be captured by the dot with, on average over all capture cycles, the same capture time, this can then be thought of as the characteristic capture time of an exciton t_{eh}. An imbalance in the number of electrons and holes can cause charged excitonic complexes, in this regime the capture time for an electron and for a hole are not the same [7]. For example a single electron and two holes creates an exciton with an extra hole in the dot, this is referred to as a positively charged exciton, or positive trion. The photoluminescence spectrum of each complex is different due to the Coulomb interaction between the carriers. The spectrum of the entire QD can be made up of many peaks, these correspond to transitions in the fine-structure. These transitions are probabilistic and can be understood by stochastic modeling [7, 8]. Identifying each peak can be done by photon correlation measurements and modeling, which will be described in Chapter 2.

1.2 Introduction to stochastic processes

A deterministic system is one in which the state of the system at time $t + \delta t$ can be fully characterised by the state of the system at time t. A stochastic system is not deterministic and only the probability of being in a certain state at a certain time is characterised (See Ref. [9] for a good introduction to stochastic systems).

If, in a stochastic system, the probability of being is state n at time t depends only on the system at time $t - \Delta t$ and not times before it then the system is said to be Markovian. For a Markovian process the joint probability distribution function is denoted as

$$P(x_1, t_1; x_2, t_2; ....; x_n, t_n) \tag{1.1}$$

Which is the probability that the system is in the state x_1 at t_1, x_2 at t_2 and state x_n at t_n for $t_1 > t_2 > \ldots > t_n$ [10].

The conditional probability distribution function is denoted as

$$P(x_1, t_1; ....; x_m, t_m \mid x_{m+1}, t_{m+1}; \ldots; x_n, t_n) \tag{1.2}$$

which is the probability that the system is in the state x_1 at time t_1 and x_m at time t_m given that it was in the state x_{m+1} at time t_{m+1} and x_n at time t_n

For a Markov process the history of the system, apart from the immediate past, has no effect on the future state of the system and thus in the continuous case

$$P(x_1,t_1;....;x_m,t_m \mid x_{m+1},t_{m+1};...;x_n,t_n) = P(x_1,t_1;....;x_m,t_m \mid x_{m+1},t_{m+1}). \quad (1.3)$$

A consequence of this is that the system can be described by only two probability distribution functions (PDF).

$$P(x_2,t_2) = \int dx_1 P(x_2,t_2 \mid x_1,t_1)P(x_1,t_1) \quad (1.4)$$

This PDF means that the probability of being in any state x_2 at time t_2 depends on the probability of being in another state x_1 at time t_1 and then transitioning into state x_2. This probability is then integrated over all other states x_1 to give the total probability. The other PDF to characterise the system is the Chapman - Kolmogorov equation

$$P(x_3,t_3 \mid x_1,t_1) = \int dx_2 P(x_3,t_3 \mid x_2,t_2)P(x_2,t_2 \mid x_1,t_1) \quad (1.5)$$

This equation implies that the conditional probability of being in state x_3 at time t_3, given the system was in state x_1 at time t_1 is given by transitioning from state x_1 to some other state x_2 and then transitioning into x_3. The total probability is given by integrating over all intermediate states x_2.

1.2.1 Markov chain.

The case when the states and time are discrete and the process is stationary will be examined here. The states will be denoted by n and m. Eq (1.4) and Eq (1.5) are written as

$$P(n_2, t_2) = \sum_{n_1} P(n_2, t_2 \mid n_1, t_1) P(n_1, t_1) \tag{1.6}$$

$$P(n_3, t_3 \mid n_1, t_1) = \sum_{n_2}^{n_1} P(n_3, t_3 \mid n_2, t_2) P(n_2, t_2 \mid n_1, t_1) \tag{1.7}$$

A stationary process is one where the conditional PDF $P(n, t \mid n', t')$ only depends on the time step Δt, here for simplification $\Delta t = 1$. The PDF $P(n, t'+k, n', t')$ can then be denoted as $p^{(k)}_{n,n'}$. The Chapman- Kolmogorov equation can then be written as

$$p^{(2)}_{n,m} = \sum_{n'} p^{(1)}_{n,n'} p^{(1)}_{n',m} \tag{1.8}$$

It is clear from this that the state of the system at time $k = 2$, $p^{(2)}_{n,m}$ is simply $p^{(2)} = (p^{(1)})^2$. Thus the time evolution of the system is given by $p^{(k)} = (p^{(1)})^k$. If R is defined as the stochastic transition matrix with elements $R_{n,n'} = p^{(1)}_{n,n'}$. Each element in R is non-negative, with each column in R summing to unity. Eq (1.6) can be written as

$$P(n, t+1) = \sum_{n'} p^{(1)}_{n,n'} P(n', t) \tag{1.9}$$

This is called a Markov chain. $P(n, t)$ is the probability of being in state n at time t and the transition probabilities are given by $p^{(1)}_{n,n'}$ which defines the probability of going from state n' to state n. If it is defined the column vector $\vec{P}(t) = P(n, t)$ the Markov chain can be written as

$$\vec{P}(t) = R^t \vec{P}(0) \tag{1.10}$$

Markov chains are presented here just for the understanding of stochastic systems and will not be used throughout the rest of the report.

1.2.2 Master equation.

A master equation is a Markov chain in the limit of time being continuous. It is a formalism that describes the probability of a system with N discrete states, being in the state n with respect to a continuous time variable t.

The Chapman - Kolmogorov equation in this form is

$$P(n, t+\delta \mid n_0, t_0) = \sum_{n'} P(n, t+\Delta t \mid n't')P(n', t \mid n_0, t_0) \tag{1.11}$$

It is assumed that $P(n, t+\delta \mid n', t)$ is of the form

$$P(n, t+\delta \mid n', t) = \begin{cases} 1 - \sum_{n \neq n''} Q(n'' \mid n)\Delta t & : n = n' \\ Q(n \mid n')\Delta t & : n \neq n' \end{cases} \tag{1.12}$$

This quantity defines the transitions into and out of the state n. The quantity $Q(n' \mid n)$ is the transition rate defined only for $n \neq n'$. Substituting into the Chapman - Kolmogorov equation gives

$$\frac{P(n, t+\Delta t \mid n_0, 0) - P(n, t \mid n_0, 0)}{\Delta t} = \sum_{n \neq n'} Q(n \mid n')P(n', t \mid n_0, 0) - \sum_{n \neq n'} Q(n' \mid n)P(n, t \mid n_0, 0) \tag{1.13}$$

Taking the limit $\Delta t \to 0$ and making the transition from $P(n, t \mid n_0, 0)$ to $P(n, t)$ gives

$$\frac{dP(n,t)}{dt} = \sum_{n \neq n'} Q(n \mid n')P(n', t) - \sum_{n \neq n'} Q(n' \mid n)P(n, t) \tag{1.14}$$

This is the master equation for a Markov process. It gives the time evolution of the probability of being in a certain state. This master equation is commonly denoted in matrix form

$$\frac{d\vec{P}}{dt} = T\vec{P} \tag{1.15}$$

Where T is a matrix made up of the transitions, it is related to the matrix R of the Markov chain by $T = \exp(R)$.

1.2.3 Solving the master equation

If given a master equation as follows

$$\frac{d\vec{P}}{dt} = T\vec{P} \tag{1.16}$$

Where $\vec{P}(t)$ is a column vector describing the probabilities of the system, the probability of being in state n is given by the $n-th$ row of $\vec{P}(t)$. T is the matrix describing the transitions into and out of each state. Define λ_n to be the eigenvalues of the transition matrix T, and $\vec{V}_n$ to be the eigenvectors given by the equation

$$T\vec{V}_n = \lambda_n \vec{V}_n \tag{1.17}$$

The time evolution of $\vec{P}(t)$ is then given by the spectral expansion solution [11]

$$\vec{P}(t) = a_1\vec{V}_1\ e^{\lambda_1 t} + a_2\vec{V}_2\ e^{\lambda_2 t} \cdots + a_n\vec{V}_n\ e^{\lambda_n t} \tag{1.18}$$

$$\vec{P}(t) = \sum_n a_n\vec{V}_n\ e^{\lambda_n t} \tag{1.19}$$

Where the coefficients a_n are given by solving the system

$$\sum_n \vec{V}_n a_n = \vec{P}(0) \tag{1.20}$$

1.3 Neutral exciton system.

A well accepted master equation [8, 7] system for the neutral exciton-biexction system is described here. p_0 is the probability of having an empty QD, p_x is the probability of the QD being occupied by an exciton and p_{xx} the probability of it being occupied by a biexciton. The upward transition, i.e. the rate of capture of excitons, is the same for the empty state and the exciton state. It is denoted here by $1/t_c$, where t_c is the characteristic capture time of an exciton. For the system examined here there is no upward transition for the biexciton state. The exicton decays to the empty state by the emission of a photon, with spontaneous emission rate $1/\tau_x$, where τ_x is the characteristic lifetime of the exciton state. The biexciton decays to the exciton state with lifetime τ_{xx}. This system is shown schematically in Figure 3.

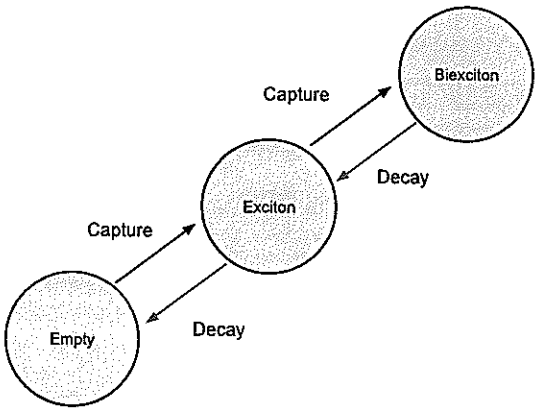

Figure 3: Schematic of the empty-exciton-biexciton Markov process.

This system can be written in a rate equation form that represents the master equations

$$\frac{dp_0}{dt} = -\frac{p_0}{t_c} + \frac{p_x}{\tau_x} \tag{1.21}$$

$$\frac{dp_x}{dt} = +\frac{p_0}{t_c} - \frac{p_x}{\tau_x} - \frac{p_x}{t_c} + \frac{p_{xx}}{\tau_{xx}} \tag{1.22}$$

$$\frac{dp_{xx}}{dt} = +\frac{p_x}{t_c} - \frac{p_{xx}}{\tau_{xx}} \tag{1.23}$$

$$\tag{1.24}$$

This system can also be written in the form

$$\frac{d\vec{P}}{dt} = T\vec{P} \tag{1.25}$$

where P is a column vector consisting of p_0, p_x and p_{xx} and T is given by

$$T = \begin{pmatrix} -\frac{1}{t_c} & \frac{1}{\tau_x} & 0 \\ \frac{1}{t_c} & -\frac{1}{t_c} - \frac{1}{\tau_x} & \frac{1}{\tau_{xx}} \\ 0 & \frac{1}{t_c} & -\frac{1}{\tau_{xx}} \end{pmatrix}. \tag{1.26}$$

This model will be analysed further and fitted to experimental data in Chapter 3.

2 Correlations

In this section the correlation between certain transitions will be analysed. For the quantum dot system explained later, it is possible to measure certain transitions in the master equation system. In the proposed excitonic Markov process, the downward transitions by radiative photon emission can be measured. For this reason a correlation function between the measured photons would be useful.

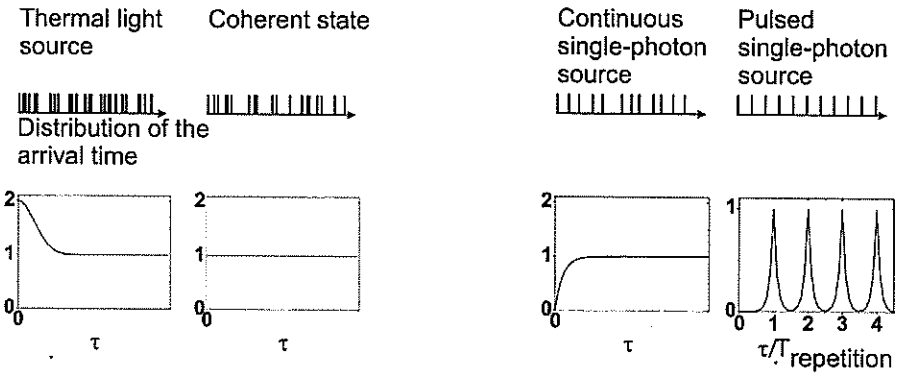

Figure 4: Example $g^{(2)}(\tau)$ for different light sources for one source beam split 50/50. [1]

This measured correlation function has the form [12]

$$g^{(2)}_{(z,y),(y,x)}(\tau) = \frac{\langle I_{z,y}(t) I_{y,x}(t+\tau)\rangle}{\langle I_{z,y}(t)\rangle \langle I_{y,x}(t+\tau)\rangle} \tag{2.1}$$

where $I_{z,y}$ is the photon from the transition from state z to state y and $I_{y,x}$ is the transition from state y to state x. Here x, y, z represent generic states and do not correspond to exciton-biexciton states as in Chapter 1.

The second order correlation function is a well known and useful idea in quantum optics (see Ref. [12] for a good introduction). For positive delay time τ it represents the conditional probability of the photon from transition $I_{y,x}$ being emitted after the photon from transition $I_{z,y}$. For negative delay time τ it represents the reverse, the conditional probability of the photon from transition $I_{z,y}$ being emitted after the photon from transition $I_{y,z}$. The $g^{(2)}(\tau)$ for some common photon sources are shown in Figure 4.

[1] Courtesy of Dr. Juska

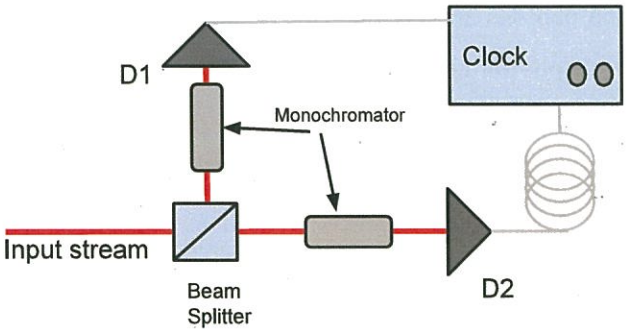

Figure 5: Schematic of a simple photon correlator.

The correlation experiment schematic is presented in Figure 5. The QD emission stream is sent towards a non-polarising 50:50 beam splitter. Photons from different transitions are energetically distinct and are discriminated using monochromators and then sent to avalanche photodiodes single photon detectors (APDs). Two APDs are used, one starts a counting module, the other stops it. The stop event is electrically delayed in order to obtain negative correlation values. The obtained curves represent the second order correlation function $g^{(2)}(\tau)$.

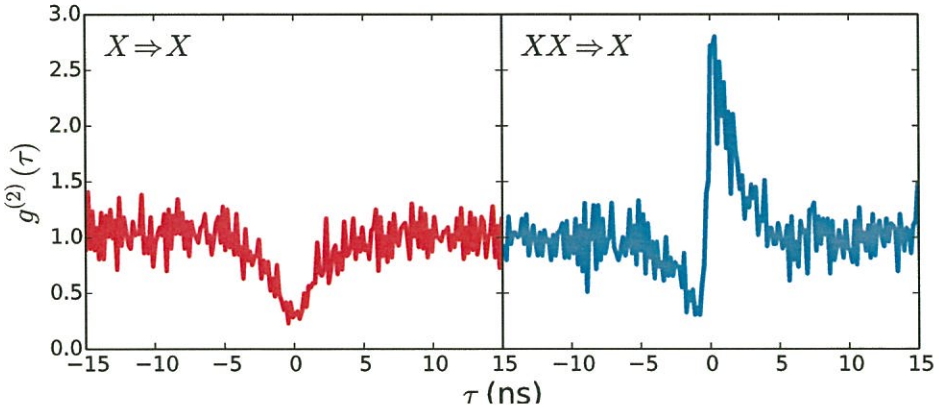

Figure 6: Correlation curves between an exciton (X) and biexciton (XX), these curves have been smoothed for clarity.

Figure 6 shows the measured exciton-exciton photon (X-X) correlation and the biexciton-exciton photon (XX-X) correlation. In the exciton-exciton case it is expected that there is decreased probability of an exciton photon being emitted quickly after an exciton photon.

When the biexciton photons are ignored, this is equivalent to regulated single photon emission and is known as photon antibunching. This decreased probability is clearly seen near $\tau = 0$ in the $X \Rightarrow X$ case in Figure 6. $g^{(2)}(0)$ is not perfectly zero as it would hopefully be, this is due to limited detector resolution and perhaps immediate re-population of the QD by some other source after emission.

In the biexciton-exciton case there is increased probability of an exciton photon being emitted after a biexciton photon is emitted, since the biexciton decays directly into the exciton, this is known as photon bunching. This increased probability is clearly seen in the $XX \Rightarrow X$ case for $\tau > 0$ in Figure 6. There is decreased probability of a biexciton photon being emitted quickly after and exciton photon, since the QD needs to capture two new excitons, and this will take some time. This decreased probability is clearly seen in the $\tau < 0$ case in the $XX \Rightarrow X$ plot.

2.1 Modeling the physical correlations

In this section the physical measurement of the correlations will be derived in the formalism of stochastic processes. Denote the set of possible states in which the QD can be at a given point in time by $S = \{0, X, XX\}$. The set of elementary events Ω is defined as the set of all functions from $\mathbb{R} \Rightarrow S$. The interpretation of this is as follows: taking one element $\omega \in \Omega$, then this element is function from $\mathbb{R} \Rightarrow S$, i.e. $\omega(t) \in S$. The physical interpretation is that if ω is the selected elementary event, then the QD is in state $\omega(t)$ for all t. The function ω therefore defines the trajectory of the QD in the set S as a function of time. Physical measurement attaches to every ω a real number, i.e. a physical measurement corresponds to a random variable. The measurement (or random variable) $I^t_{z,y}$ considered here detects, whether or not a photon corresponding to a transition from z to y arrives in a time interval $[t, t + \delta]$ where δ is a small number determined by the time resolution of the detector.

Based on ω, this transition event can be formally defined through

$$I^t_{z,y} : \Omega \to \{0,1\} \tag{2.2}$$

$$I^t_{z,y} : (\omega(t) = z) \ \wedge \ (\omega(t + \Delta t) = y) \tag{2.3}$$

This map takes on the value 1 if the transition did occur in the time range, and the value 0 if it did not. The probability of this event occurring is then denoted by $\langle I_{z,y} \rangle$.

- $I^{t_1}_{z,y}$ is the event of the emission of the photon when transitioning from state z to state y in some interval $[t_1, t_1 + \delta]$.
- $I^{t_2}_{y,x}$ which is the event from state y to state x in some interval $[t_2, t_2 + \delta]$.

The absolute probability of these events occurring is

$$\langle I_{z,y} \rangle = p(y, t + \delta \mid z, t)p(z, t) = p(y, \delta \mid z, 0)p_s(z) \tag{2.4}$$

$$\langle I_{y,x} \rangle = p(x, \alpha \mid y, 0)p_s(y) \tag{2.5}$$

Case $\tau > 0$. There are two cases that are important when relating to the measurement. In the case when the delay time $\tau > 0$ the transitions are measured in reverse order. The measurement is of the conditional probability that $I_{y,x}$ occurs given that the event $I_{z,y}$ occurred. The cascade of events is as follows

- The system is in the state z at time t, the probability of this occurring is $p_s(z)$ i.e. the stationary probability of being in z.
- Then the transition from z at time t to state y at time $t + \epsilon$, the probability of this occurring is $p(y, t + \epsilon \mid z, t)$.
- Then the system stays in state y for time τ, the probability of staying is $p(y, t + \tau + \epsilon \mid y, t + \epsilon)$.
- Then finally the system transitions from y to state x, the probability of this transition is $p(x, t + \tau + \epsilon + \alpha \mid y, t + \tau + \epsilon)$.

The total probability of this cascade occurring is given by

$$\langle I^t_{z,y} \mid I^{t+\tau}_{y,x} \rangle = p(x, t+\tau+\epsilon+\alpha \mid y, t+\tau+\epsilon)p(y, t+\tau+\epsilon \mid y, t+\epsilon)p(y, t+\epsilon \mid z, t)p_s(z) \quad (2.6)$$

The correlation function $g^{(2)}(\tau)$ can be written, in the limit $\alpha \to 0$ and $\epsilon \to 0$ as

$$g^{(2)}_{(z,y),(y,z)}(\tau) = \frac{p(y, t+\tau \mid y, t)}{p_s(y)}, \quad \tau > 0 \quad (2.7)$$

Case $\tau < 0$. In the case when the delay time $\tau < 0$ the transitions are measured in reverse order. The measurement is of the conditional probability that $I_{z,y}$ occurs given that the event $I_{y,x}$ occurred. The cascade of events is as follows

- The system is in the state y at time $t+\tau+\epsilon$ (for negative τ), the probability of this being the case is $p_s(y)$.
- Then the transition from y at time $t+\tau+\epsilon$ to state x at time $t+\tau+\epsilon+\alpha$, the probability of this occurring is $p(x, t+\tau+\epsilon+\alpha \mid y, t+\tau+\epsilon)$.
- Then the system transitions from state x at time $t+\tau+\epsilon+\alpha$ to state z at t, the probability of this is $p(x, t+\tau+\epsilon+\alpha \mid z, t)$.
- Then finally the system transitions from z to state y, the probability of this transition is $p(y, t+\epsilon \mid z, t+\epsilon)$.

The total probability of this cascade occurring is

$$\langle I^t_{y,x} \mid I^{t+\tau}_{z,y} \rangle = p(y, t+\epsilon \mid z, t)p(z, t \mid x, t+\tau+\epsilon+\alpha)p(x, t+\epsilon+\tau+\alpha \mid y, t+\tau+\epsilon)p_s(y) \quad (2.8)$$

The correlation function $g^{(2)}(\tau)$ can be written, in the limit $\alpha \to 0$ and $\epsilon \to 0$

$$g^{(2)}_{(z,y),(y,z)}(\tau) = \frac{p(z, t+\tau \mid x, t)}{p_s(y)}, \quad \tau < 0 \quad (2.9)$$

2.2 Adapting the model to the experimental data.

2.2.1 Response function of the detectors

When a photon hits the detectors its arrival time lies on an interval defined by the gaussian response function of the detectors.

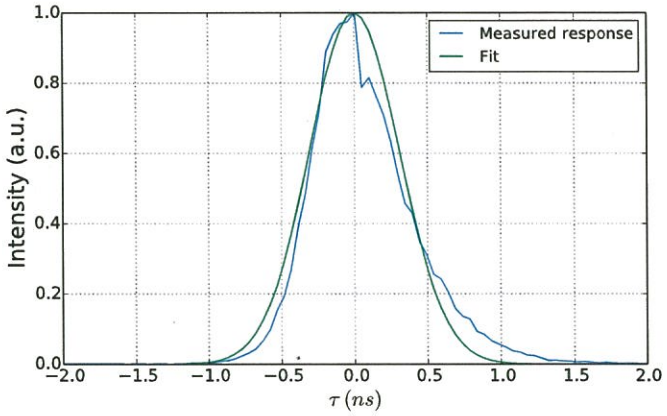

Figure 7: Measured response function of the detectors with a fitted Gaussian.

The measurement of this response function involved sending the same signal towards both APD's and is shown in Figure 7. In the ideal case case this curve would be a Dirac delta function at $\tau = 0$, however due to the detector resolution the function is broadened. This measured response function was fitted and the FWHM was determined to be 0.73 ns.

2.2.2 Describing measured correlations as single exponentials

The solution of the master equation can be written as the sum of exponential functions as a first approximation it was checked whether a single exponential dominates in the measured results,

$$\vec{P}(t) = \sum_n a_n \vec{V}_n \, e^{\lambda_n t} \approx a_d \vec{V}_d \, e^{\lambda_d t} \tag{2.10}$$

Where the λ_d implies the dominant eigenvalue, $\vec{V}_d$ the dominant eigenvector and a_d the dominant coefficient. If this is the case then the second order correlation function can be approximately written as

$$g^{(2)}(\tau) = 1 + \begin{cases} c_p \exp(-\lambda_p \tau) & \tau > 0 \\ c_n \exp(\lambda_n \tau) & \tau \leq 0 \end{cases} \tag{2.11}$$

Where λ_p (λ_n) is the dominant eigenvalue on the $\tau > 0$ ($\tau < 0$) scale, and c_p (c_n) the dominant fitting coefficient on the $\tau > 0$ ($\tau < 0$) scale, given by $c_p = a_p \vec{V}_{p,i}$ ($c_n = a_n \vec{V}_{n,i}$), where i is the row of the eigenvector corresponding to the measured state. This would simplify the fitting procedure. Single exponential functions were fitted to the data in order to see if this is valid.

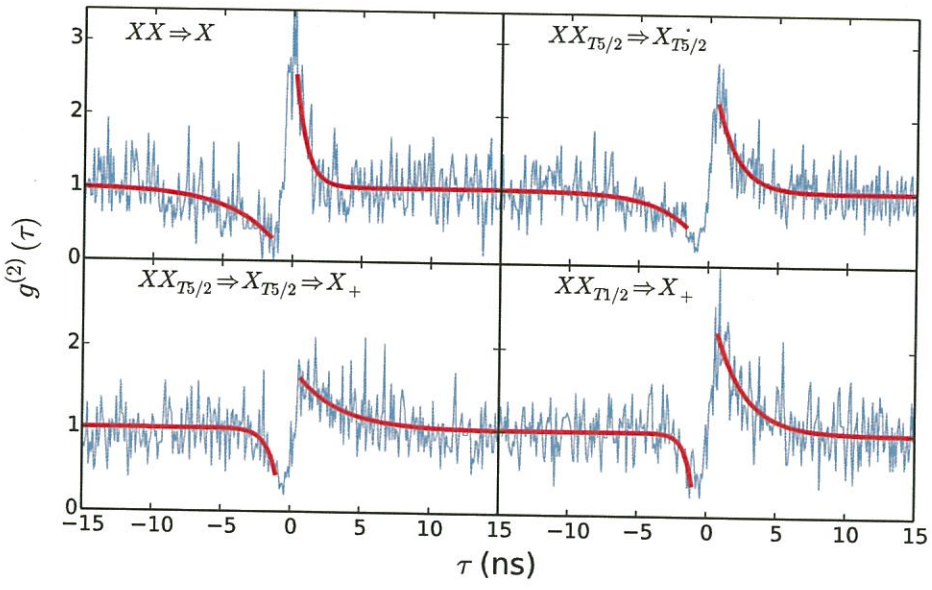

Figure 8: Single exponentials fitted to the positive and negative τ for some example measured correlation curves.

Figure 8 shows the fitted exponentials, the fitting parameters are unimportant as of yet. This is simply to show that a $g^{(2)}(\tau)$ described by single exponentials can be a good first approximation to the reality.

2.2.3 Convolution

From the previous section an approximate $g^{(2)}(\tau)$ can be defined as single exponentials.

$$g^{(2)}(\tau) = 1 + \begin{cases} c_1 \exp(-\lambda_1 \tau) & \tau > 0 \\ c_2 \exp(\lambda_2 \tau) & \tau \leq 0 \end{cases} \tag{2.12}$$

In order to fit this $g^{(2)}(\tau)$ to the experimental data it must be convoluted with the response function of the detectors. The convolution of two functions $f(t)$ and $g(t)$ is defined as

$$[f * g](\tau) = \int_{-\infty}^{\infty} f(t) g(\tau - t) \mathrm{d}t \tag{2.13}$$

The convolution of $g^{(2)}(\tau)$ with a Gaussian is defined as

$$g_c^{(2)}(\tau) = \frac{1}{\sqrt{2\pi\sigma^2}} \int_{-\infty}^{\infty} g^{(2)}(t) \exp(\frac{-(\tau - t)^2}{2\sigma^2}) \mathrm{d}t \tag{2.14}$$

Where FWHM $= 2\sqrt{2 \ln 2}\ \sigma$. Thus $\sigma = 0.3$ ns since FWHM $= 0.73$ns. Considering the definition of $g_c^{(2)}(\tau)$, it can be written as the sum of two integrals.

$$g_c^{(2)}(\tau) = \frac{1}{\sqrt{2\pi\sigma^2}} \left(\int_0^{\infty} g_+^{(2)}(t) \exp(\frac{-(\tau - t)^2}{2\sigma^2}) \mathrm{d}t + \int_{-\infty}^{0} g_-^{(2)}(t) \exp(\frac{-(\tau - t)^2}{2\sigma^2}) \mathrm{d}t \right) \tag{2.15}$$

$$= 1 + \frac{1}{\sqrt{2\pi\sigma^2}} \left(c_1 \int_0^{\infty} \exp(-\lambda_1 t) \exp(\frac{-(\tau - t)^2}{2\sigma^2}) \mathrm{d}t + c_2 \int_{-\infty}^{0} \exp(\lambda_2 t) \exp(\frac{-(\tau - t)^2}{2\sigma^2}) \mathrm{d}t \right)$$

Looking at the argument of the exponentials:

$$\lambda t + \frac{(t - \tau)^2}{2\sigma^2}$$

$$\lambda t + \frac{\tau^2}{2\sigma^2} - \frac{2t\tau}{2\sigma^2} + \frac{t^2}{2\sigma^2}$$

$$\tau\lambda - \frac{1}{2}\sigma^2\lambda^2 + \frac{(t-\tau+\sigma^2\lambda)^2}{2\sigma^2}$$

Introducing the change of variable $s = t - \tau \pm \sigma^2\lambda_{1,2}$. Thus $\mathrm{d}s = \mathrm{d}t$. In the positive case limits become: $(-\tau + \sigma^2\lambda_1, \infty)$, in the negative case the limits become $(-\infty, -\tau - \sigma^2\lambda_2)$

$$\begin{aligned} g_c^{(2)}(\tau) = 1 &+ \frac{1}{\sqrt{2\pi\sigma^2}} c_1 \exp\left(-\lambda_1\tau + \frac{1}{2}\sigma^2\lambda_1^2\right) \cdot \int_{-\tau+\sigma^2\lambda_1}^{\infty} \exp\left(-\frac{s^2}{2\sigma^2}\right) \mathrm{d}s \\ &+ \frac{1}{\sqrt{2\pi\sigma^2}} c_2 \exp\left(\lambda_2\tau + \frac{1}{2}\sigma^2\lambda_2^2\right) \cdot \int_{-\infty}^{-\tau-\sigma^2\lambda_2} \exp\left(-\frac{s^2}{2\sigma^2}\right) \mathrm{d}s \end{aligned} \tag{2.16}$$

Introducing another change of variable $y = s/\sqrt{2\sigma^2}$, with $\mathrm{d}s = \sqrt{2\sigma^2}\mathrm{d}y$ and the limits rescale.

$$\begin{aligned} g_c^{(2)}(\tau) = 1 &+ c_1\sqrt{2\sigma^2} \exp\left(-\lambda_1\tau + \frac{1}{2}\sigma^2\lambda_1^2\right) \cdot \int_{-\frac{\tau}{\sqrt{2\sigma^2}}+\frac{\sigma\lambda_1}{\sqrt{2}}}^{\infty} \exp\left(-y^2\right) \mathrm{d}y \\ &+ c_2\sqrt{2\sigma^2} \exp\left(\lambda_2\tau + \frac{1}{2}\sigma^2\lambda_2^2\right) \cdot \int_{-\infty}^{-\frac{\tau}{\sqrt{2\sigma^2}}-\frac{\sigma\lambda_2}{\sqrt{2}}} \exp\left(-y^2\right) \mathrm{d}y \end{aligned} \tag{2.17}$$

In the second integral change the limits to $(\frac{\tau}{\sqrt{2\sigma^2}} + \frac{\sigma\lambda_2}{\sqrt{2}}, \infty)$ and replace y with $-y$.

$$\begin{aligned} g_c^{(2)}(\tau) = 1 &+ c_1\sqrt{2\sigma^2} \exp\left(-\lambda_1\tau + \frac{1}{2}\sigma^2\lambda_1^2\right) \cdot \int_{-\frac{\tau}{\sqrt{2\sigma^2}}+\frac{\sigma\lambda_1}{\sqrt{2}}}^{\infty} \exp\left(-y^2\right) \mathrm{d}y \\ &+ c_2\sqrt{2\sigma^2} \exp\left(\lambda_2\tau + \frac{1}{2}\sigma^2\lambda_2^2\right) \cdot \int_{+\frac{\tau}{\sqrt{2\sigma^2}}+\frac{\sigma\lambda_2}{\sqrt{2}}}^{\infty} \exp\left(-y^2\right) \mathrm{d}y \end{aligned} \tag{2.18}$$

Then introducing the complementary error function.

$$\mathrm{erfc}(x) = \frac{2}{\sqrt{\pi}} \int_x^{\infty} \exp\left(-t^2\right) dt$$

$$g_c^{(2)}(\tau) = 1 + \frac{c_1\sqrt{2\pi\sigma^2}}{2}\exp\left(-\lambda_1\tau + \frac{1}{2}\sigma^2\lambda_1^2\right)\operatorname{erfc}\left(-\frac{\tau}{\sqrt{2\sigma^2}} + \frac{\sigma\lambda_1}{\sqrt{2}}\right) + \frac{c_2\sqrt{2\pi\sigma^2}}{2}\exp\left(\lambda_2\tau + \frac{1}{2}\sigma^2\lambda_2^2\right)\operatorname{erfc}\left(+\frac{\tau}{\sqrt{2\sigma^2}} + \frac{\sigma\lambda_2}{\sqrt{2}}\right) \tag{2.19}$$

This is the final result. In the case of a positive time bunched $g^{(2+)}(\tau)$, we have $c_2 = -1$. In the case of all time anti-bunched $g^{(2-)}(\tau)$, we have $c_1 = c_2 = -1$. $g_c^{(2)}(\tau)$ is continious and differentiable. It would be interesting to see what $g_c^{(2+)}(\tau)$ looks like at $\tau = 0$.

$$g_c^{(2)}(0) = 1 + \frac{c_1\sqrt{2\pi\sigma^2}}{2}\exp\left(\frac{1}{2}\sigma^2\lambda_1^2\right)\operatorname{erfc}\left(\frac{\sigma\lambda_1}{\sqrt{2}}\right) + \frac{c_2\sqrt{2\pi\sigma^2}}{2}\exp\left(\frac{1}{2}\sigma^2\lambda_2^2\right)\operatorname{erfc}\left(\frac{\sigma\lambda_2}{\sqrt{2}}\right) \tag{2.20}$$

It is seen that whether $g_c^{(2+)}(0)$ is less than or greater than unity depends on the relative values of c_1, λ_1 and λ_2.

This function $g_c^{(2)}(\tau)$ will be used in the next chapter to fit to measured photon correlation data.

3 Application of the model

3.1 Simple three level system.

In this section the model that has been developed will be applied to measured data. The emission spectrum for this QD is presented in Figure 9 (a) taken at increasing excitation powers [13]. The hypothesised exciton (X) and biexciton (XX) transition peaks are labeled in the plot and correspond to transitions in the fine structure shown in Figure 9 (b).

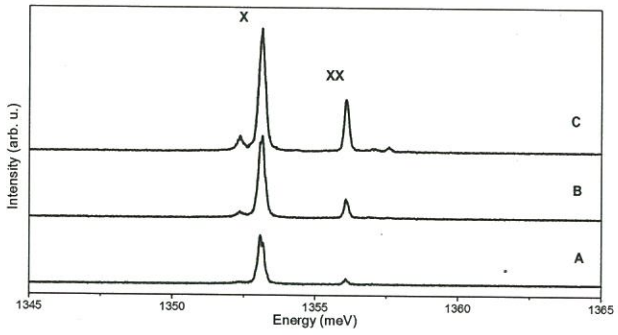

(a) [2]

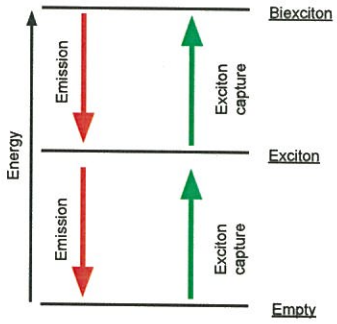

(b)

Figure 9: (a) Spectrum taken at increasing excitation power and (b) fine structure of an empty - exciton - biexciton system.

This fine structure can be modeled by the neutral excitonic system described in Chapter 1, by the transition matrix

$$T = \begin{pmatrix} -\frac{1}{t_c} & \frac{1}{\tau_x} & 0 \\ \frac{1}{t_c} & -\frac{1}{t_c} - \frac{1}{\tau_x} & \frac{1}{\tau_{xx}} \\ 0 & \frac{1}{t_c} & -\frac{1}{\tau_{xx}} \end{pmatrix}. \tag{3.1}$$

Here τ_x (τ_{xx}) is the characteristic decay lifetime of the exciton (biexciton) and t_c is the characteristic capture time of an exciton. τ_x and τ_{xx} can be directly measured. By syncing a laser pulse to a start clock and the photon detection event stops the clock, the time depen-

[2] Courtesy of Dr. Pelucchi/Dr. Juska

dent photo-luminescent spectrum can be built up. Fitting this time dependent spectrum with an exponential decay will give the characteristic decay lifetime of the state. These curves are shown for the exciton and biexciton in Figure 10.

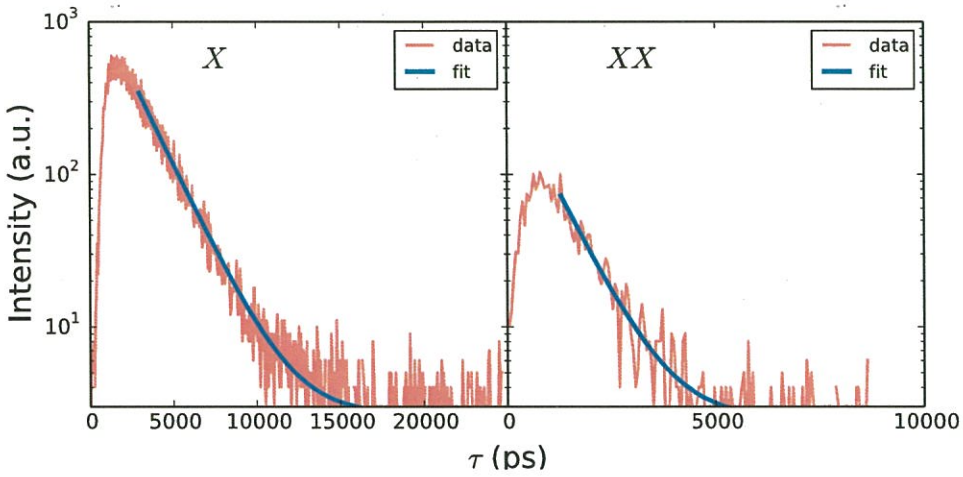

Figure 10: Time resolved intensity of the exciton (X) and biexciton (XX) emission for a pulse starting at $\tau = 0$ ($\log_{10}$ scale). [3]

The fitted lifetimes were deduced to be $\tau_x = 1.85 \pm 0.04$ ns and $\tau_{xx} = 0.79 \pm 0.05$ ns. The only free parameter then when fitting the model to the data is the capture time t_c.

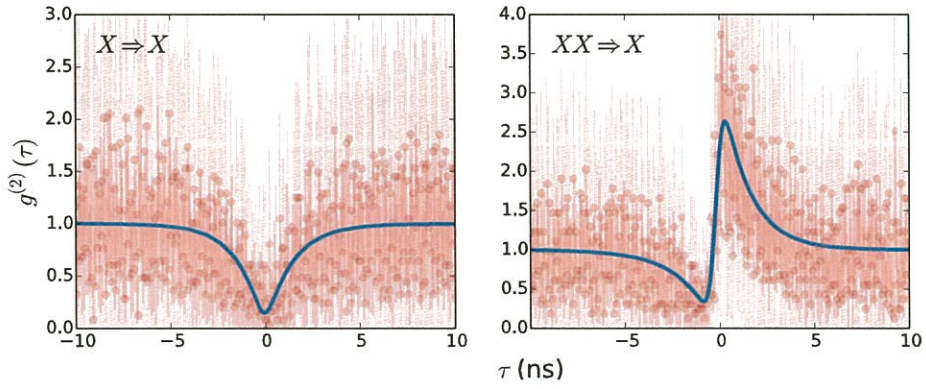

Figure 11: Measured and fitted exciton-exciton (X-X) and biexciton-exciton (XX-X) correlation curves. [4]

The fitting of the $g_c^{(2)}(\tau)$ derived in Chapter 2 was done with Scientific Pythons [14] (`scipy`)

[3] Courtesy of Dr. Juska

[4] Data courtesy of Dr. Pelucchi/Dr. Juska

`curve_fit` routine, which does a weighted non-linear least squares fit. The weights in this case were given by $1/\sqrt{y}$, where y is the $\hat{y}$ axis data, $\sqrt{y}$ is the typical Poisson deviation. The routine returns the best fit parameters and the covariance matrix. The standard errors are given by the square root of the diagonals of the covariance matrix. These measured results and fits are shown in Figure 11. The data was normalised by the total y axis average and the absolute count rates were $\sim$ 20 counts per bin at the end of the experiment, $\sim$ 5000 total per second on the detectors distributed over many bins. The error bars on the measured results are given by $y \pm \sqrt{y}$, which were calculated before normalisation, which is typical for a Poisson process. In Figure 11 the blue line traces the fitted curve, the red dots are the data points and the red lines are the error bars for each point (the darker red are simply overlapping overlapping lines).

Parameter	Fit	Error
λ_1	0.7	$\pm$ 0.2
λ_2	0.7	$\pm$ 0.2

Table 1: Exciton-exciton correlation fit, shown in Figure 11 (a).

As in Chapter 2, λ_1 is the exponential argument of $g^{(2)}(\tau)$ for $\tau > 0$, and λ_2 is the exponential argument for $\tau < 0$. As seen in Table 1 λ_1 equal to λ_2 to within the error, this is expected since the exciton-exciton correlation should be antibunching and symmetric.

Parameter	Fit	Error
c_1	2.5	$\pm$ 0.3
λ_1	0.7	$\pm$ 0.1
λ_2	0.54	$\pm$ 0.1

Table 2: Biexciton-exciton correlation fit, shown in Figure 11 (b).

In the biexciton-exciton case the results are presented in Table 2. c_1 is the intensity coefficient in the $\tau > 0$ time scale, and λ_1, λ_2 are defined as before. Again λ_1 is close to λ_2 within the error, which is expected and discussed in the next few paragraphs.

[4] Data courtesy of Dr. Pelucchi/Dr. Juska

In order to relate these values to the transition matrix T first the eigenvalues of T must be discussed. Using $\tau_x = 1.85$ ns and $\tau_{xx} = 0.79$ ns along with an ansatz value of $t_c = 3$ ns the transition matrix is then given by

$$T = \begin{pmatrix} -0.36 & 0.54 & 0 \\ 0.36 & -0.89 & 1.26 \\ 0 & 0.35 & -1.26 \end{pmatrix}. \tag{3.2}$$

The matrix T should have all non-negative entries, and the columns should sum to unity. The eigenvalues of T are $\lambda_{T1} = 0$, $\lambda_{T2} = -0.69$ and $\lambda_{T3} = -1.83$. It has eigenvectors

$$\vec{V}_1 = \begin{pmatrix} -0.84 \\ 0.80 \\ 0.29 \end{pmatrix}, \ \vec{V}_2 = \begin{pmatrix} -0.51 \\ 0.51 \\ -0.8 \end{pmatrix}, \ \vec{V}_3 = \begin{pmatrix} -0.13 \\ -0.29 \\ 0.50 \end{pmatrix}. \tag{3.3}$$

It would seem that since λ_{T2} is not at all close to the $\lambda_{1,2}$ from the fittings, that the $\lambda_{1,2}$ must be equivalent to λ_{T1}, this is why all the measured $\lambda_{1,2}$ would have similar values to λ_{T1} and seen in Table 1 and Table 2. Using the eigenvectors of T and calculating the coefficients a the $g^{(2)}(\tau > 0)$ solution (as defined in Chapter 2) can be deduced.

$$p_{x,x}(t) = a_{T1}\vec{V}_{T1(x,x)}\mathrm{e}^{\lambda_{T1}t} + a_{T2}\vec{V}_{T2(x,x)}\mathrm{e}^{\lambda_{T2}t} + a_{T3}\vec{V}_{T3(x,x)}\mathrm{e}^{\lambda_{T3}t} \tag{3.4}$$

Where $\vec{V}_{(xx)}$ is the eigenvector component corresponding to the xx state. The $\lambda_{T1} = 0$ is significant because it gives the steady state probability distribution, given by $p_s(x) = a_{T1}\vec{V}_{T1}\mathrm{e}^{\lambda_{T1}t} = a_{T1}\vec{V}_{T1}\mathrm{e}^0$. For $\tau > 0$, after normalisation by $p_s(x)$, the solution is then given by,

$$g^{(2)}(\tau) = 1 - 0.73\ \mathrm{e}^{-0.69\tau} - 0.27\ \mathrm{e}^{-1.83\tau} \tag{3.5}$$

As discussed in Chapter 1 the coefficients a_n are given by solving

$$\sum_n \vec{V}_n \vec{a}_n = \vec{P}(0) \tag{3.6}$$

Where $\vec{P}(0)$ is the column vector representing the initial probabilities of the stochastic system. In this case the a_n are normalised by the steady state coefficient a_0, this gives $a_1/a_0 = -0.73$ and $a_2/a_0 = -0.27$. Since the correlation is symmetric about $\tau = 0$, there is no difference between $\tau > 0$ and $\tau < 0$. The theoretical $g^{(2)}(\tau)$ is then given by

$$g^{(2)}(\tau) = 1 - 0.73\ \mathrm{e}^{-0.69|\tau|} - 0.27\ \mathrm{e}^{-1.83|\tau|} \tag{3.7}$$

This needs to be compared with the fitted $g^{(2)}(\tau)$, with $\lambda_1 = \lambda_2 = 0.7$ ns of

$$g^{(2)}_{fit}(\tau) = 1 - \mathrm{e}^{-0.7|\tau|} \tag{3.8}$$

Applying the approximation that the physical $g^{(2)}(\tau)$ are described by single exponentials only, then the theoretical $g^{(2)}(\tau)$ should be described by either

$$g^{(2)}_1(\tau) = 1 - 0.73\ \mathrm{e}^{-0.69|\tau|} \tag{3.9}$$

or

$$g^{(2)}_2(\tau) = 1 - 0.27\ \mathrm{e}^{-1.83|\tau|} \tag{3.10}$$

Plotting these post convolution is presented in Figure 12. It is clear that $g^{(2)}_1(\tau)$ is most like the fitted result. However, it does not dip to such a low $g^{(2)}(0)$ as the fit, this is satisfactory because $g^{(2)}_1(0) + g^{(2)}_2(0) = 0$, which will match the fit. It can be thought of that both the behavior of $g^{(2)}_1(\tau)$ and $g^{(2)}_2(\tau)$ are important to characterise $g^{(2)}(0)$. Then $g^{(2)}_2(\tau)$ dies out quickly and $g^{(2)}_1(\tau)$ dominates at $\tau \neq 0$.

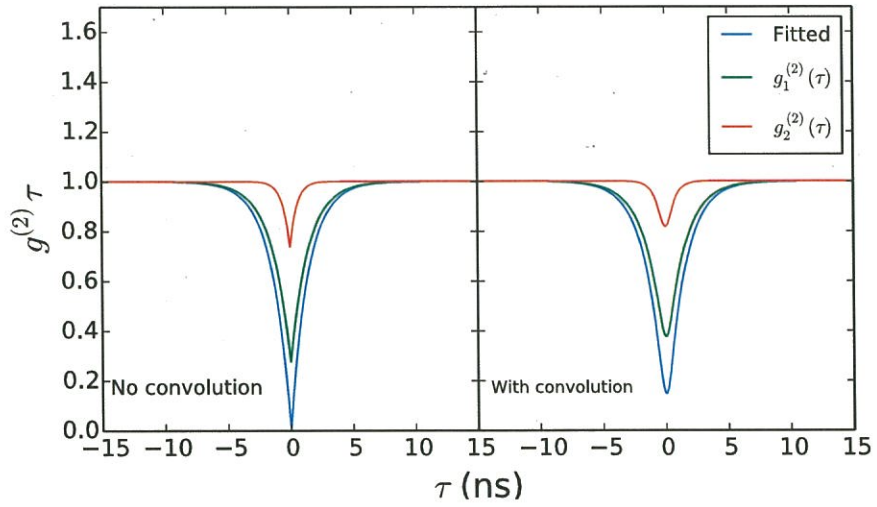

Figure 12: Exciton-exciton photon correlation function $g^{(2)}(\tau)$ derived from the ansatz transition matrix T.

This analysis then permits the choice of one of the eigenvalues of T to be $\lambda_{T1} = \lambda_1 = 0.7 \pm 0.2\ \text{ns}^{-1}$. This will be checked now again by looking at the biexciton-exciton photon cross correlation.

In the theoretical biexciton-exciton case, by solving the master equation of the T with an ansatz $t_c = 3$ ns the $g^{(2)}(\tau)$ is given by

$$g_T^{(2)}(\tau) = 1 + \begin{cases} 0.68\ \mathrm{e}^{-0.69\tau} + 1.11\ \mathrm{e}^{-1.83\tau} & \tau > 0 \\ -1.61\ \mathrm{e}^{-0.69\tau} + 0.61\ \mathrm{e}^{-1.83\tau} & \tau \leq 0 \end{cases} \tag{3.11}$$

In this case, as a first approximation, the $g^{(2)}(\tau)$ is split into the components made up of each eigenvalue component.

$$g_1^{(2)}(\tau) = 1 + \begin{cases} 0.68\ \mathrm{e}^{-0.69\tau} & \tau > 0 \\ -1.61\ \mathrm{e}^{-0.69\tau} & \tau \leq 0 \end{cases} \tag{3.12}$$

and

$$g_2^{(2)}(\tau) = 1 + \begin{cases} 1.11\ \mathrm{e}^{-1.83\tau} & \tau > 0 \\ 0.61\ \mathrm{e}^{-1.83\tau} & \tau \leq 0 \end{cases} \tag{3.13}$$

The correlation functions are plotted along with the fitted function in Figure 13. It is clear from these plots that the theory does not exactly match the fitted values. It seems that more "intensity", i.e. larger coefficients are needed in the $g_1^{(2)}(\tau)$ curve. However the corresponding λ_{T1} has good agreement with the fitted λ_1. Also $g^{(2)}(0^+)$ in the fitted case is 3.5, and $g_1^{(2)}(0^+) + g_2^{(2)}(0^+) = 2.79$, which are of the same order. These are evaluated at $g^{(2)}(0^+)$ and not $g^{(2)}(0)$ because the anti bunching peak will have a contribution at $\tau = 0$.

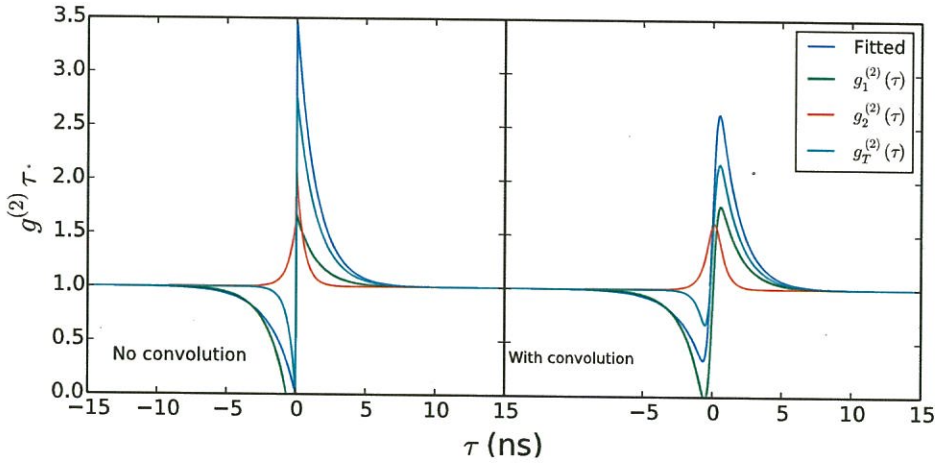

Figure 13: Biexciton-exciton photon correlation function $g^{(2)}(\tau)$ derived from the ansatz transition matrix T.

It is taken then that $\lambda_{T1} = \lambda_1 = 0.7 \pm 0.2\ \mathrm{ns}^{-1}$. Only one eigenvalue is needed to determine the proper t_c since τ_x and τ_{xx} have been measured independently. It is left now to find the t_c which gives a $\lambda_{T1} = 0.7 \pm 0.2\ \mathrm{ns}^{-1}$.

Figure 14 shows the eigenvalue λ_{T1} plotted versus t_c, for fixed τ_x and τ_{xx}. The black bars are the represent the error in the fitted λ_1, of $0.7 \pm 0.2\ \mathrm{ns}^{-1} \Rightarrow [0.68, 0.72]$. The range of t_c which falls in this interval is calculated to be $[2.4, 2.9]$ ns with an optimal value of $t_c = 2.6$ ns. An interval is presented and not an errer because λ_{T1} is not linear on this range as seen in the Figure.

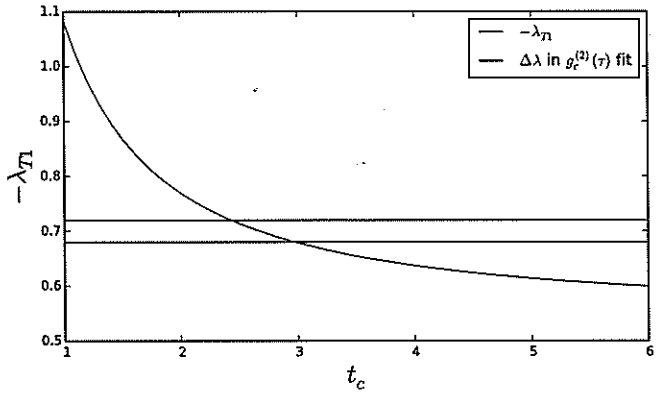

Figure 14: Eigenvalue λ_{T1} of the transition matrix T plotted versus t_c, for set τ_x and τ_{xx}.

The matrix T is then fully characterised by

$$T = \begin{pmatrix} -\frac{1}{t_c} & \frac{1}{\tau_x} & 0 \\ \frac{1}{t_c} & -\frac{1}{t_c} - \frac{1}{\tau_x} & \frac{1}{\tau_{xx}} \\ 0 & \frac{1}{t_c} & -\frac{1}{\tau_{xx}} \end{pmatrix}. \tag{3.14}$$

where $\tau_x = 1.85$ ns, $\tau_{xx} = 0.79$ ns and $t_c = 2.6$ ns on the interval $[2.4, 2.9]$ ns.

4 Conclusions and further work

It has been suggested in Ref. [15] that the biexciton - exciton measurements presented in this chapter may not actually be true. That the system is really a biexciton - negatively charge exciton system. This was checked by altering the charging of the QD by utilising a second excitation laser. A negatively charged exciton would behave much like a neutral exciton in the auto correlation measurements, but not so in the biexciton - negatively charged exciton cross correlation measurements. This could explain the lower "intensity" (coefficients) in the theorised $g^{(2)}(\tau)$ curves in Figure 13.

Further work needs to be done on the methods presented in Chapter 3. A more robust statistical method for fitting the model to the data needs to be developed. If, for a given hypothesised fine-structure, a minimal set of correlation measurements could be developed to fully chategorise the transition matrix it would be tremendously useful. Understanding capture parameters and emission spectrum is vital to creating technology from QDs.

In conclusion, in this report the relationship between the Markov master equation and the commonly used second order correlation function has been defined. An approximate fitting model was derived and this model was then tentatively applied to data. This fitting procedure needs to be developed further.

References

[1] Oliver Benson, Charles Santori, Matthew Pelton, & Yoshihisa Yamamoto. *Regulated and Entangled Photons from a Single Quantum Dot.* Phys. Rev. Lett. 84, 2513 (2000).

[2] G. Juska, V. Dimastrodonato, L. O. Mereni, A. Gocalinska & E. Pelucchi. *Towards quantum-dot arrays of entangled photon emitters.* Nature Photonics 7, 527–531 (2013).

[3] P. Michler, A. Kiraz, C. Becher, W. V. Schoenfeld, P. M. Petroff, Lidong Zhang, E. Hu, A. Imamoglu. *A Quantum Dot Single-Photon Turnstile Device.* Science. 290, 2282-2285 (2000).

[4] R. M. Stevenson, C. L. Salter, J. Nilsson, A. J. Bennett, M. B. Ward, I. Farrer, D. A. Ritchie, & A. J. Shields *Indistinguishable Entangled Photons Generated by a Light-Emitting Diode.* Phys. Rev. Lett. 108, 040503 (2012).

[5] M. A. Nielsen & I. L. Chuang. *Quantum Computation and Quantum Information. Chapter 2.* Cambridge University Press (2000).

[6] R. M. Thompson, R. M. Stevenson, A. J. Shields, I. Farrer, C. J. Lobo, D. A. Ritchie, M. L. Leadbeater, & M. Pepper *Single-photon emission from exciton complexes in individual quantum dots.* Phys. Rev. B. 64, 201302 (2001)

[7] M. H. Baier, A. Malko, E. Pelucchi, D. Y. Oberli, & E. Kapon. *Quantum-dot exciton dynamics probed by photon-correlation spectroscopy.* Phys. Rev. B 73, 205321 (2006).

[8] M. Grundmann & D. Bimberg. *Theory of random population for quantum dots.* Phys. Rev. B 55, 9740 (1997).

[9] C. W. Gardiner *Handbook of stochastic methods Third edition.* Springer 2004. ISBN 3-540-20882-8

[10] A. Amann *AM4062 lecture notes.* (2014).

[11] Isi Mitrani & Ram Chakka *Spectral expansion solution for a class of Markov models: application and comparison with the matrix-geometric method.* Performance Evaluation 23, 241-260 (1995).

[12] M. Fox *Quantum Optics, an introduction. Chapter 6.* Oxford University Press (2006).

[13] G. Juska *Pyramidal quantum dots: single and entangled photon sources and correlation studies.* Thesis, University College Cork (2014).

[14] Eric Jones and Travis Oliphant and Pearu Peterson and others, SciPy: Open source scientific tools for Python, 2001–, http://www.scipy.org/

[15] G. Juska, **E. Murray**, V. Dimastrodonato, T. H. Chung, A. Gocalinska & E. Pelucchi *Entangled photon emission from (111)B site-controlled Pyramidal quantum dots.* Submitted to Phys. Rev. B. (2014).